Choice of South Asian Summer Monsoon Indices*

Bin Wang and Zhen Fan
Department of Meteorology, University of Hawaii at Manoa, Honolulu, Hawaii

ABSTRACT

In the south Asian region, two of the major precipitation maxima associated with areas of intensive convective activity are located near the Bay of Bengal and in the vicinity of the Philippines. The variations of monthly mean outgoing longwave radiation in the two regions are poorly correlated, particularly in the decade of 1980s. The enhanced convection over the Bay of Bengal and Indian subcontinents is coupled with reinforced monsoon circulation west of 80°E over India, the western Indian Ocean, and the tropical northern Africa. In contrast, the enhanced convection in the vicinity of the Philippines corresponds to intensified monsoon circulation primarily east of 80°E over southeast Asia including the Indochina peninsula, South China Sea, Philippine Sea, and the Maritime Continent. To better reflect regional monsoon characteristics, two convection indices (or associated circulation indices that are dynamically coherent with the convection indices) are suggested to measure the variability of the Indian summer monsoon (ISM) and the southeast Asian summer monsoon, respectively.

The change in the Bay of Bengal convection (the ISM) has planetary-scale implications, whereas the change in Philippine convection has primarily a regional impact including a linkage with the east Asia subtropical monsoon. The equatorial western Pacific winds exhibit a considerably higher correlation with the ISM convection than with the Philippine convection. During the summers when a major Pacific warm episode occurs (e.g., 1982–83, 1986–87, 1991–92, and 1997), the convection and circulation indices describing the ISM often diverge considerably, causing inconsistency among various normally coherent monsoon indices. This poses a primary difficulty for using a single monsoon index to characterize the interannual variability of a regional monsoon. The cause of the breakdown of the coherence between various convection and circulation indices during ENSO warm phase needs to be understood.

1. Introduction

The year-to-year variation of the Asian monsoon is one of the strongest signals of the earth's climate variability. Its interaction with ENSO has been of great interest to the climate research community. In order to quantify the variability of the south Asian summer monsoon (SASM), it is appealing to use a representative variable (or variables) as an objective measure (or measures), if such variables exist. The Southern Oscillation index provides an excellent example of quantifying a complex phenomenon using a single parameter. Using concise and meaningful indices to characterize monsoon variability can greatly facilitate empirical studies of the relationship between monsoon variability and lower boundary forcing. It can also aid objective assessment of the capability of numerical models in reproducing monsoon variability. The choice of proper monsoon indices has recently received exceptional attention and has developed notable controversy (Webster and Yang 1992; Goswami et al. 1999; Ailikun and Yasunari 1998; Lau 1998; Kawamura 1998). The purpose of this paper is to draw the attention of the meteorological community to this perplexing and sometimes confusing problem.

The All Indian Summer Rainfall Index (hereafter AIRI) has long been used as a measure of the Indian summer monsoon (ISM), which is defined by the seasonally averaged precipitation over all the Indian sub-

*School of Ocean and Earth Science and Technology Publication Number 4759.

Corresponding author address: Dr. Bin Wang, Department of Meteorology, University of Hawaii, 2525 Correa Road, Honolulu, HI 96822.
E-mail: bwang@soest.hawaii.edu

In final form 16 September 1998

divisions from June to September 1871–1995 (Parthasarathy et al. 1992; Parthasarathy et al. 1995). AIRI has been widely used in the studies of the ISM and ENSO or tropical biennial oscillation (e.g., Shukla and Paolino 1983; Meehl 1987; Shukla and Mooley 1987; Yasunari 1991). While AIRI is a good indicator of the strength of the monsoon rain over India, it is not clear how well it represents the large-scale summer monsoon in south Asia.

To reflect the variability of the broad-scale SASM, Webster and Yang (1992) used a circulation index that is defined by a time-mean zonal wind (U) shear between 850 and 200 hPa, $U850–U200$, averaged over south Asia from the equator to 20°N and from 40° to 110°E (hereafter WYI). The WYI and AIRI sometimes give disparate measures of the monsoon strength. For instance, AIRI in 1988 was nearly two standard deviations above the normal, whereas WYI is only slightly positive (Parthasarathy et al. 1995; Krishnamurti et al. 1989). In a recent manuscript, Ailikun and Yasunari (1998) showed that the WYI is associated with the convective activity over the western Pacific rather than over the south Asian monsoon region. They concluded that the WYI and AIRI represent completely different monsoon and circulation fields in the Asian/western Pacific monsoon region. The above conclusion was made based on the data from 1979–95 during which AIRI and WYI were poorly correlated (Goswami et al. 1999).

The weak correlation between AIRI and WYI motivated Goswami et al. (1999) to focus on the rainfall averaged over a larger region (10°–30°N, 70°–110°E), which covers not only the Indian subcontinent but also the northern Bay of Bengal and a portion of south China. They found that the extended rainfall index is well correlated with a Monsoon Hadley Circulation Index (hereafter MHI), which is defined by the meridional wind (V) shear between 850 and 200 hPa ($V850–V200$) averaged over the same area as the extended rainfall index. The MHI also exhibits a better correlation with AIRI than WYI does.

The choice of an index is, by definition, somewhat arbitrary. To quantify complex large-scale monsoon characteristics using a single index is often difficult. It requires understanding of the essential physics governing the monsoon variability. Our focus is placed on understanding the dynamical basis for adequate choice of meaningful indices that characterize year-to-year variations of the large-scale SASM. For this purpose, we will first identify action centers for the SASM in terms of convection and circulation fields (section 2), then establish empirical relationships between the variations in the convective action centers and monsoon circulations (section 3). These relationships provide a basis for defining dynamically coherent monsoon indices and for explaining the linkages and differences among various monsoon indices, which are defined using different variables and are averaged over different regions. The understanding gained from these analyses leads to a recommendation for choice of Asian summer monsoon indices (section 4).

2. Action centers of the south Asian summer monsoon

Convection variability is estimated using outgoing longwave radiation (OLR) from 1974 to 1997 (with a 10-month gap in 1978) derived originally from National Oceanic and Atmospheric Administration (NOAA) satellite observations (Gruber and Krueger 1984) and calibrated by Waliser and Zhou (1997). This dataset is longer than other satellite estimations of rainfall, although it is not necessarily the best due to being contaminated by cirrus cloud, surface topographical influence, etc. The monthly mean Climate Prediction Center Merged Analysis of Precipitation (CMAP) was used to double-check the results derived using OLR. The CMAP is constructed by merging several kinds of information sources with different characteristics, including gauge observations, estimates inferred from a variety of satellite observations, and National Centers for Environmental Prediction–National Center for Atmospheric Research (NCEP–NCAR) reanalysis (Xie and Arkin 1997). Over the tropical Indian and western Pacific Oceans the correlation coefficient between the monthly mean negative OLR and CMAP exceeds 0.7, while over the Indian subcontinent the correlation coefficient is largely between 0.5 and 0.7 (figure not shown). For the regions of our concern (see next section), OLR provides a meaningful estimation of large-scale convective variability on monthly to seasonal timescales. The circulation data (850- and 200-hPa zonal and meridional winds) used in this study are derived from the NCEP–NCAR reanalysis for the period from January 1958 to December 1997 (Kalnay et al. 1996). The 850- and 200-hPa winds are classified as A-type variables, which are strongly influenced by observed data and are thus the most reliable class.

To define an index, we focus on the key regions where either the summer monsoon rainfall or the 850-

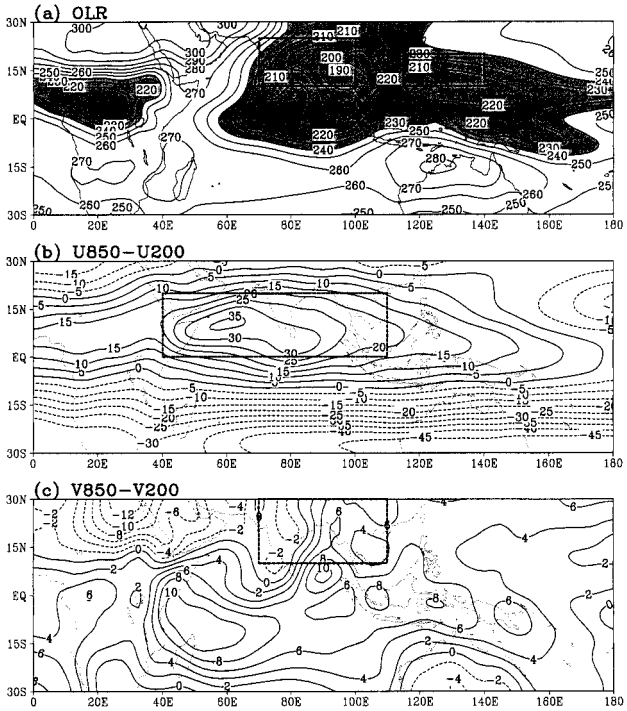

FIG. 1. Seasonal (Jun–Sep) mean maps of (a) OLR, (b) zonal, and (c) meridional vertical shears (defined as 850-hPa wind minus 200-hPa wind). The OLR climatology is derived for the period 1974–97 with a 10-month gap in 1978. The wind climatology is derived for the period 1958–97 from NCEP–NCAR reanalysis. The unit of contour values is W m^{-2} for OLR, and m s^{-1} for vertical shear. The boxes in (a), (b), and (c) represent, respectively, the regions in which the convective indices CI1 and CI2 in this paper, the Webster and Yang index (WYI), and the meridional Hadley index (MHI) are defined. For definitions of CI1 and CI2 refer to Table 1.

and 200-hPa winds display maximum intensity (termed action centers). Figure 1 illustrates geographic distributions of seasonal- (June–September) mean OLR, and zonal and meridional vertical shears (defined as 850-hPa wind minus 200-hPa wind). There are two principal convection centers; one is located in the Bay of Bengal and the other in the vicinity of the Philippines (Fig. 1a). They are indicated by the lowest OLR centers with seasonal-mean values below 200 and 210 W m^{-2}, respectively. These convection centers are also atmospheric heat sources identified by the diagnostic study of Yanai and Tomita (1998).

In view of the critical role of convective latent heat release in driving the summer monsoon, we define two convective indices to quantify the intensity change of the convective heating: the convection index 1 (CI1) and convection index 2 (CI2), which are defined by the negative OLR anomalies (with respect to the climatological annual cycle) averaged, respectively, over the Bay of Bengal–India region (10°–25°N, 70°–100°E) and in the vicinity of the Philippines (10°–20°N, 115°–140°E) (the two regions are outlined in Fig. 1a). The choices of these key regions are not only based on the OLR minimum but also with reference to CMAP maximum rainfall and maximum annual range. The annual range of rainfall reflects fundamental characteristics of the monsoon rain. For convenience, we term CI1 and CI2 as convection indices for the ISM and the southeast Asian summer monsoon (SEASM), respectively.

From a circulation perspective, the monsoon is dominated by the lowest baroclinic mode, which is stimulated by the latent heat released in the middle troposphere. The vertical shears defined by the difference of 850- and 200-hPa zonal winds, U850–U200, provided a first-order approximation to the strength of the gravest baroclinic mode. Figure 1b shows that the large zonal (westerly) vertical shears in pressure coordinates, denoted by WS (westerly shear), extend along 10°N from Africa to the western North Pacific with a maximum of 36 m s^{-1} (10°N, 60°E). The WYI defined by the WSs averaged in the area (0°–20°N,

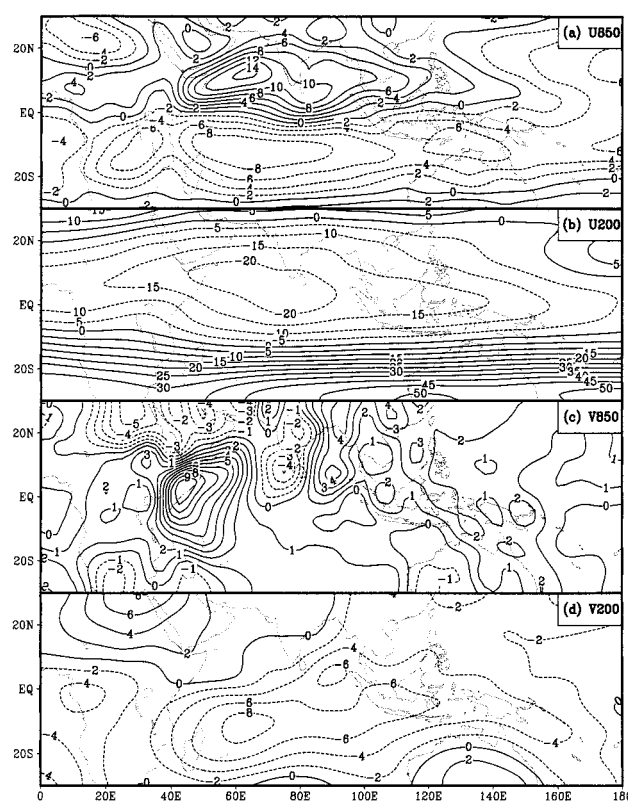

FIG. 2. Same as in Fig. 1 except for (a) 850-hPa zonal wind, (b) 200-hPa zonal wind, (c) 850-hPa meridional wind, and (d) 200-hPa meridional wind. The unit for contour values is m s^{-1}. Note different contour intervals in different panels.

40°–110°E) is thus an excellent measure of the variability of the entire SASM in terms of the zonal wind vertical shear. Note that the WYI also represents very well the strength of both the low-level (850 hPa) westerly jet and upper-level (200 hPa) easterly jet, because they nearly coincide (Figs. 2a and 2b).

The situations with meridional wind shear are different. The 200-hPa maximum northerlies are not well aligned with 850-hPa maximum southerlies. The 200-hPa strongest northerlies are found in the near-equatorial region from east of Madagascar across the Indian Ocean to the Indonesian archipelago (Fig. 2d). The maximum southerlies at 850 hPa are located primarily over the east coast of tropical Africa with a secondary maximum over the southern Bay of Bengal (Fig. 2c). The former is associated with cross-equatorial flow, whereas the latter reflects the monsoon trough over the Bay of Bengal (Fig. 2c). The strong southerlies at 850 hPa are influenced by orography and land–sea distribution, while the 200-hPa northerlies are associated with the giant Tibetan high. This is one of the reasons why the 200-hPa maximum northerlies are not well aligned with 850-hPa maximum southerlies. The meridional wind shear shown in Fig. 1c is primarily attributed to the 200-hPa cross-equatorial northerlies, except near the east coast of equatorial Africa and the head of the Bay of Bengal where the low-level monsoon southerlies dominate. Because of the significant phase difference between the upper- and lower-tropospheric meridional winds, caution must be exercised when using southerly wind shear, $V850-V200$, to quantify monsoon intensity. The MHI is defined by the southerly shear averaged over the region (10°–30°N, 70°–110°E), which is not located at the action center of the meridional vertical shear. In addition, the southerly shear in that region reverses its sign between the east and west portions of the chosen domain (Fig. 1c).

3. Relationships between the convection and circulation variabilities

To understand the meaning of AIRI, WYI, and MHI and to search for dynamically coherent monsoon indices, it is advantageous to establish the empirical relationship between the variations in convection centers and the surrounding circulation anomalies in the SASM domain. Figure 3 shows the correlation maps of the winds (the zonal and meridional winds at 850 and 200 hPa) with reference to the convection over the

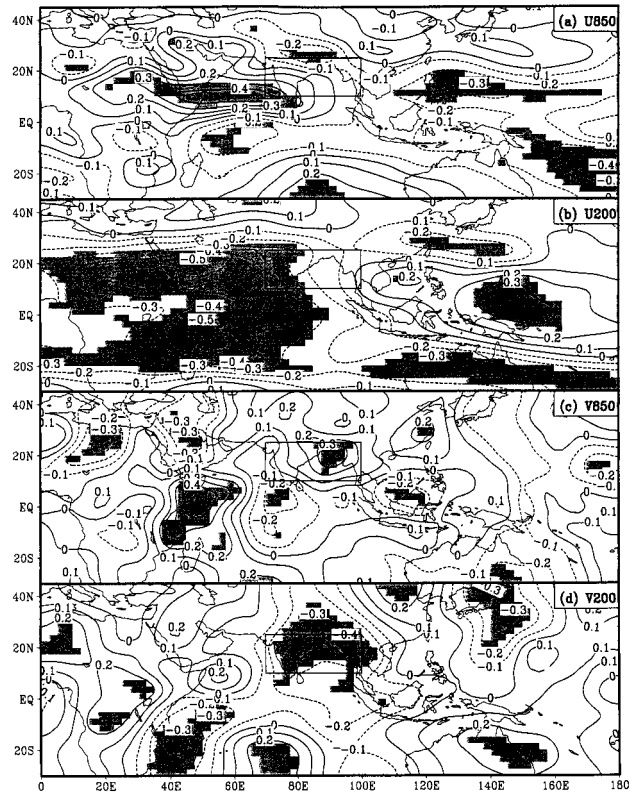

FIG. 3. Maps of correlation coefficients of zonal winds at (a) 850 hPa and (b) 200 hPa, and meridional winds at (c) 850 hPa and (d) 200 hPa with respect to convection index CI1. The calculation is based on monthly mean from Jun to Sep 1974–97 (1978 missing). Coefficients that are significant at the 95% confidence level are shaded. The definition of CI1 refers to Table 1. The boxes outline the region where CI1 is defined.

Bay of Bengal and the Indian subcontinent (10°–25°N, 70°–100°E), or the ISM convection index CI1. Note that positive CI1 (negative OLR) means enhanced convection. Statistically significant correlations at the 95% confidence level are shaded in Fig. 3. In the statistical significance test, the degrees of freedom were estimated for each grid using the method described by Livezey and Chen (1983). Figure 3 indicates that the enhanced convection over the ISM (CI1) corresponds to intensified 850-hPa westerlies in a narrow band between 5° and 15°N over the Arabian Sea (Fig. 3a), and enhanced 200-hPa easterlies over the western tropical Indian Ocean in a wide latitude band from 20°S to 25°N and tropical northern Africa (Fig. 3b). Note that the CI1 is also positively correlated with 850-hPa easterly anomalies over the Philippine Sea and 200-hPa westerly anomalies northeast of New Guinea. The enhanced convection over the Indian monsoon region (CI1) is also correlated with the magnified 850-hPa Somalia jet near the coast of Somalia,

the southerlies over the Bay of Bengal (Fig. 3c), and the 200-hPa northerlies over the Bay of Bengal and Indian subcontinent (Fig. 3d).

In response to the enhanced convection over the Bay of Bengal and the Indian subcontinent, the westerly vertical shear, *U*850–*U*200, strengthens to the west of 80°E, especially over the latitude band between 5° and 20°N from the Arabian Sea to tropical northeast Africa (Fig. 4a); whereas the southerly shear, *V*850–*V*200, is reinforced primarily in the following two regions: (a) along the east coast of Africa (the cross-equatorial flow to the southwest of the convection) and (b) over the head of the Bay of Bengal–northeast India (southerly shear over and to the east of the convection region) (Fig. 4b). It can be seen from Fig. 4b that the MHI defined by Goswami et al. (1999) using the southerly shear averaged in the region (10°–30°N and 70°–100°E) does correlate well with CI1.

The correlation maps with reference to the convection index in the vicinity of the Philippines (10°–20°N, 115°–140°E), the CI2, display quite different pictures (Fig. 5). Corresponding to enhanced convection over the Philippines, the regions of strengthened 850-hPa westerlies and 200-hPa easterlies are primarily confined to the east of 80°E. The enhanced 850-hPa westerlies occur in a narrow latitude belt between 5° and 15°N from the Philippines to Malaysia with a tail extending westward to southern India and the Arabian Sea (Fig. 5a). The intensified 200-hPa easterlies are found in a broad region around the Maritime Continent (Fig. 5b). The enhanced 850-hPa southerlies and 200-hPa northerlies are also limited to the east of 80°E (Figs. 5c,d).

The westerly shear, which best correlates with the enhanced Philippine convection, is located in southeast Asia (0°–10°N, 90°–130°E) of the southwest of the convection region (Fig. 6a). The southerly shear that best couples the enhanced Philippine convection occurs in a region extending from the eastern equatorial Indian Ocean across the Maritime Continent to the Philippine Sea (Fig. 6b). In particular, the enhanced low-level southerlies are found to the southwest of the enhanced convection (cross-equatorial flow west of Sumatra) and to the east of the enhanced convection (Fig. 5c). The cross-equatorial southerly shears are much weaker than those associated with the CI1.

One feature common to both Figs. 4c and 6c is that the enhanced westerly shears are located to the west and southwest of the correspondingly enhanced convection, while the enhanced southerly shears occur

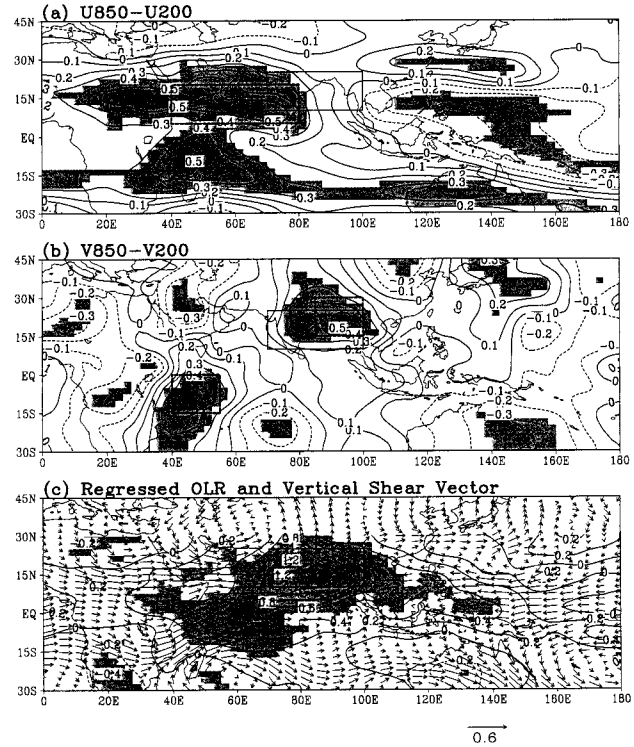

FIG. 4. Maps of correlation coefficients of (a) westerly shear (*U*850–*U*200) and (b) southerly shear (*V*850–*V*200) with respect to convection index CI1, (c) regressed negative OLR, and vertical shear vector (850-hPa wind minus 200-hPa wind) ($m^3\ s^{-1}\ W^{-1}$) with respect to CI1. Correlations in (a) and (b) and OLR regressions in (c) that are significant at the 95% confidence level are shaded. The thick dotted boxes in (a) and (b) indicate regions where the westerly shear index WSI1 and southerly shear index SSI1 are defined. The definition of CI1 refers to Table 1. Thin solid-line boxes indicate the region where CI1 is defined.

over the eastern part of the enhanced convection as well as to its southwest—the cross-equatorial shear flows (Figs. 4c and 6c). This spatial structure of the anomalous monsoon circulations (vertical shears) can be understood in terms of simple models such as Webster (1972) and Gill (1980). The cyclonic vertical shear anomalies poleward and westward of the enhanced convection and the associated cross-equatorial vertical shears result from Rossby wave dispersion in response to the anomalous heat source implied by the enhanced convection. The regressed vertical shear vector anomalies shown in Figs. 4c and 6c are therefore dynamically coherent with the large-scale convection indices CI1 and CI2, respectively.

The conspicuous differences between Figs. 4c and 6c deserve more discussion. First, the change in the ISM convection has planetary-scale implications while that in the Philippine convection has only a regional

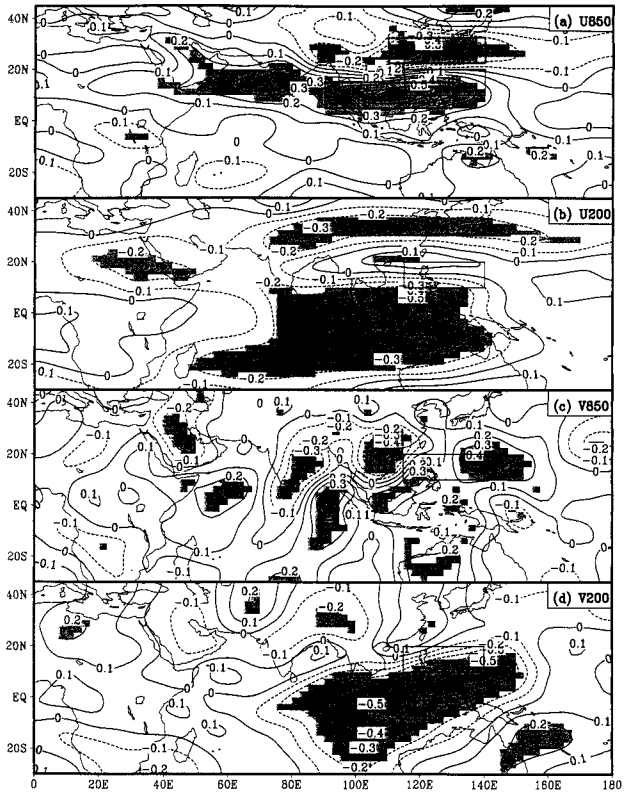

FIG. 5. The same as Fig. 3 except the correlation is computed with respect to the convection index CI2. The definition of CI2 refers to Table 1. The thick-dotted box in (a) outlines the region of DU2. Thin solid-line boxes indicate the region where CI2 is defined. DU2 is the *U*850 hPa in (5°–15°N, 90°–130°E) minus *U*850 hPa in (22.5°–32.5°N, 110°–140°E).

impact. The OLR anomalies significantly correlated with the ISM convection index, CI1 (shaded area in Fig. 4c), cover a vast area of south Asia, the north Indian Ocean, and notably the equatorial western Indian Ocean, whereas the OLR anomalies significantly correlated with CI2 occupy a much more limited area, mainly the South China Sea and the Philippine Sea (Fig. 6c). Significant vertical shear anomalies associated with CI1 tend to spread over the entire Eastern Hemisphere Tropics (Fig. 4c), whereas the vertical shear anomalies associated with CI2 is restricted to southeast Asia between 90° and 140°E (Fig. 6c). Second, the zonal shear anomalies, associated with CI1 display an east–west dipole pattern; that is, the shears are out of phase between the western Indian Ocean and the western Pacific (Fig. 4a), whereas the zonal shear anomalies associated with CI2 exhibit a north–south wave train pattern (Fig. 6a). When convection is stronger than normal over the ISM region, the low-level westerlies and upper-level easterlies weaken in the remote western Pacific from 140°E to the date line (Figs. 3a and 3b). We note that the equatorial western Pacific winds are influenced by the fluctuation in the ISM more significantly than that in the SEASM. On the other hand, when convection is stronger than normal over the Philippines, the low-level westerlies and upper-level easterlies weaken to the north of the convection in southeast China and north of the Philippines between 20° and 30°N (Figs. 5a and 5b).

Why is the ISM more influential over the western Pacific? Why do responses to variations in CI1 and CI2 display different dipole patterns? A clue lies in the fact that the convection anomalies associated with the Bay of Bengal convection (CI1) have a considerable equatorial component across the entire Indian Ocean and the northern Maritime Continent (Fig. 4c), which can effectively change the Walker circulation through eastward emanation of the equatorial Kelvin waves, forming the east–west dipole circulation anomaly and consequently affecting remote, equatorial western Pacific regions. On the other hand, the convection anomalies associated with Philippine convection (CI2) are confined to a narrow, off-equatorial latitude belt

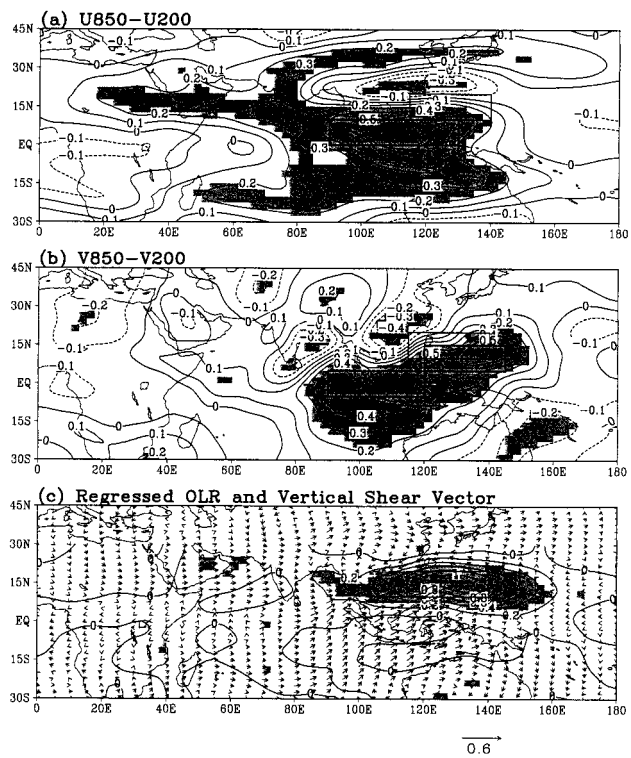

FIG. 6. The same as Fig. 4 except the correlation is computed with respect to the convection index CI2. The thick dotted boxes in (a) and (b) indicate regions where the westerly shear index WSI2 and southerly shear index SSI2 are defined. The definition of CI2 refers to Table 1. Thin solid-line boxes indicate the region where CI2 is defined.

centered at 15°N (Fig. 6c), which can effectively change the local Hadley circulation through emanation of the Rossby waves, including the wave trains emanating poleward. The latter imply that the change of Philippine Sea convection may affect the western Pacific subtropical high and the east Asia subtropical monsoon. This poleward wave train pattern was found previously by Nitta (1987) and Huang and Lu (1989).

It is interesting to observe that the OLR and monsoon shear anomalies associated with the two convection indices tend to be separable but complementary in their geographic locations (Figs. 4 and 6). This implies that the variability of westerly shear in the WYI domain (0°–20°N, 40°–110°E; shown in Fig. 1b) is attributed to the variations in both the Bay of Bengal and Philippine convection centers. It also implies that the variability of the southerly shear in the MHI domain (shown in Fig. 1c) is caused by the variation in the Bay of Bengal convection (Fig. 4b) but has little to do with Philippine convection (Fig. 6b).

4. Recommendations and discussion

a. Recommendations

The linear correlation coefficient between the convection indices CI1 and CI2 is low (0.17) and statistically insignificant at the 95% confidence level. The low correlation between CI1 and CI2 is particularly evident during the 1980s, for example, 1980, 1981, 1983, 1984, 1985, and 1988 (Fig. 7). This suggests that the monthly mean convection in the two summer monsoon regions vary more or less independently. We, therefore, recommend two indices, the convection indices CI1 and CI2, be used to characterize the interannual variations of the ISM and the SEASM, respectively.

The regional characteristics of the ISM and SEASM (including the Philippine Sea) are not only reflected by the convection–circulation relationships (Figs. 4 and 6) but also revealed by the onset patterns of the rainy season. Figure 8 is a blowup picture modified from Fig. 4a of Wang (1994). The south Asian rainy season starts from Malaysia–Thailand in late April and shifts progressively later *northwestward* toward northwestern India in the ISM domain but progressively later *northeastward* toward the western North Pacific in the SEASM domain. On the intraseasonal timescale, the convection over the ISM and the Philippine Sea tends to be out of phase (Lau and Chan 1986; Zhu and Wang 1993). Based on the characteristic monsoon evolution with respect to the forcing arising from anomalous sea surface temperatures and land surface processes, Lau (1998) has recently suggested distinguishing the south Asian and southeast Asian monsoon subsystems in the tropical Asian monsoon domain.

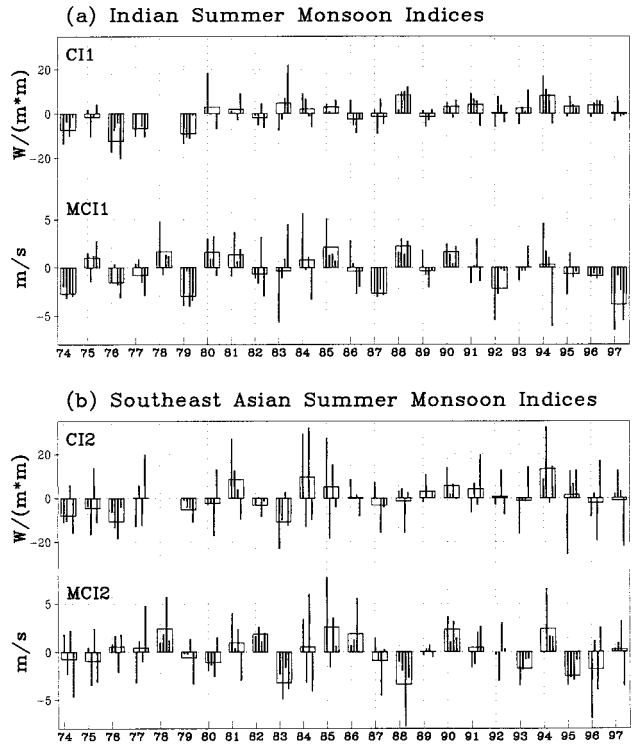

FIG. 7. The monthly (bars) and seasonal (boxes) mean (Jun–Sep 1974–97) monsoon convection and circulation indices for the (a) Indian summer monsoon and (b) southeast Asian summer monsoon. The vertical tick marks point to June of each year.

The coherent dynamical structures between the circulation and convection anomalies (Figs. 3, 4, 5, 6)

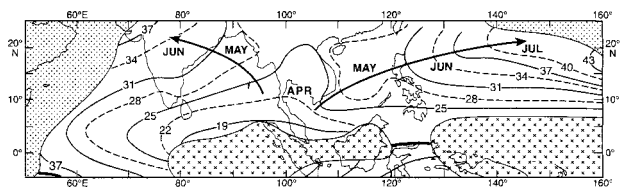

FIG. 8. Phase diagram for the onset of local rainy season computed using the climatological pentad mean OLR (subject to a five-pentad running mean) at each 2.5 × 2.5 grid point. The solid contours are isochrones with labels indicating the Julian pentad during which the rainy season begins. Light meshed shading areas are dry areas where climatological pentad-mean OLR is higher than 230 W m^{-2} all year around. Dark meshed shading areas represent regions with a year-round pentad-mean OLR lower than 230 W m^{-2}. The onset of the rainy season is defined by the first pentad when the pentad-mean OLR becomes lower than 240 W m^{-2}.

suggest that the two convection indices, CI1 and CI2, used for the ISM and SEASM can also represent the respective large-scale circulation anomalies. In view of the longer circulation data records and some advantages using circulation indices (Webster and Yang 1992), it is desirable to construct circulation indices for the ISM and SEASM, respectively. These circulation indices make it possible to extend the monsoon index back to 1958 using NCEP–NCAR reanalysis data.

Based on the empirical relationships between convection and vertical shear anomalies (Figs. 4 and 6) and the characteristic Rossby wave response to an off-equatorial heat source, one may select westerly shears to the southwest of the convection and southerly shears in the eastern part of the convection region and in the cross-equatorial flow regions as monsoon circulation indices. To explore this line of thinking, the ISM circulation indices corresponding to the convection index CI1 can be defined using either westerly shear averaged over (5°–20°N, 40°–80°E) (hereafter WSI1) or southerly shear averaged over the combined regions of (15°–30°N, 85°–100°E) and (0°–15°S, 40°–55°E) (hereafter SSI1). The thick dotted boxes shown in Figs. 4a and 4b indicate the regions over which WSI1 and SSI1 are defined. Similarly, the SEASM circulation indices corresponding to the convection index CI2 can be defined by the westerly shear averaged over the area (0°–10°N, 90°–130°E) (hereafter WSI2), or southerly shear averaged over the combined areas (5°–15°N, 120°–145°E) and (5°S–5°N, 90°–120°E) (hereafter SSI2). The thick dotted boxes shown in Figs. 6a and 6b indicate the regions over which WSI2 and SSI2 are defined. Notice that unlike the ISM, in the SEASM region the 200-hPa wind and 850-hPa wind anomalies are not vertically aligned (Fig. 2). Therefore, the vertical shear indices may not be an adequate index for the SEASM. For this reason, we constructed an additional circulation index using 850-hPa winds, that is, the difference between the westerly anomalies averaged over (5°–15°N, 90°–130°E) and the westerly anomalies averaged over (22.5°–32.5°N, 110°–140°E), signified by DU2. The construction of this index is based on the empirical relation shown in Fig. 5a and the low-level Rossby wave response to the heat source in the vicinity of the Philippines. The index DU2 represents lower-tropospheric vorticity anomalies associated with the convective index CI2.

Table 1 lists the correlation coefficients between various SASM convection and circulation indices. The convection index CI1 in the ISM region is well correlated with the westerly shear over the Arabian Sea, the WSI1, and the southerly shear over the Bay of Bengal (15°–30°N, 85°–100°E) and the east coast of equatorial Africa (0°–15°S, 40°–55°E), the SSI1. On the other hand, the convection index over the Philippines, CI2, is well correlated with DU2 and SSI2 (Table 1). Note also that the correlation between the ISM indices and the SEASM indices are generally low and unreliable. The good correlations between the indices CI1 and WSI1 (or SSI1) and between CI2 and DU2 (or SSI2) suggest that WSI1/SSI1 and DU2/SSI2 are meaningful alternative indices for the ISM and the SEASM, respectively. As mentioned earlier, however, the southerly shear should be used with caution because the meridional shears do not represent well the first baroclinic mode stimulated by the convective heating,

TABLE 1. Correlation coefficients between various south Asian summer monsoon indices. The calculation is based on monthly mean from June to September of 1974–97 (1978 missing). Coefficients that are significant at the 99% confidence level are bolded. CI1 and CI2 are negative OLR anomalies averaged over the area (10°–25°N, 70°–100°E) and (10°–20°N, 115°–140°E), respectively. WSI1 and WSI2 are westerly shears (*U*850–*U*200) averaged over the area (5°–20°N, 40°–80°E) and (0°–10°N, 90°–130°E), respectively. SSI1 is the southerly shears (*V*850–*V*200) averaged over the combined areas (15°–30°N, 85°–100°E) and (0°–15°S, 40°–55°E). SSI2 is the southerly shears averaged over the combined areas (5°S–5°N, 90°–120°E) and (5°–15°N, 120°–145°E). DU2 is the *U*850 in (5°–15°N, 90°–130°E) minus *U*850 in (22.5°–32.5°N, 110°–140°E).

	CI1	WSI1	SSI1	CI2	DU2	SSI2	WSI2
CI1	1.00	**0.61**	**0.67**	0.17	–0.17	0.09	–0.12
WSI1	**0.61**	1.00	**0.63**	**0.29**	0.13	0.12	**0.33**
SSI1	**0.67**	**0.63**	1.00	0.00	–0.23	–0.19	–0.06
CI2	0.17	**0.29**	0.00	1.00	**0.72**	**0.70**	**0.59**
DU2	–0.17	0.13	–0.23	**0.72**	1.00	**0.66**	**0.81**
SSI2	0.09	0.12	–0.19	**0.70**	**0.66**	1.00	**0.48**
WSI2	–0.12	**0.33**	–0.06	**0.59**	**0.81**	**0.48**	1.00

especially since the SSI2 is dominated by upper-tropospheric circulation anomalies and strongly influenced by the south Asia subtropical high. For this reason and for the reason of simplicity, we recommend WSI1 and DU2 be the monsoon circulation index for the ISM and the SEASM, respectively, and will denote them simply by MCI1 and MCI2, respectively.

Table 2 presents correlation coefficients among the proposed circulation indices (MCI1 and MCI2) and the existing indices. The correlation coefficients are computed using monthly mean data during boreal summer from June to September for the 40-yr period from 1958 to 1997 except for the coefficients with AIRI, which are calculated using seasonal (June–September) means for the period of 1958–95. The AIRI and MHI are well correlated with MCI1, but not the MCI2, indicating that AIRI and MHI are measures of ISM but not the SEASM. On the other hand, the WYI not only highly correlates with MCI1 (the correlation coefficient is 0.93), but also correlates, to a certain degree, with MCI2 (the correlation coefficient is 0.35). In this sense, the WYI primarily reflects the monsoon variability of the ISM but also, to some extent, the variability of the SEASM. It should be noted, however, that the westerly shears induced by the two convection centers tend to cancel each other over the western Pacific and southeast Asia (Figs. 4c and 6c). In addition, the correlation between the circulation indices MCI1 and MCI2 is low (0.15) and not significant at the 90% confidence level. The WYI does not reflect different regional monsoon characteristics well. This weakness can be seen from its relatively low correlations with AIRI (0.52), MHI (0.29), and MCI2 (0.35).

TABLE 2. Correlation coefficients between various south Asian summer monsoon indices. Calculations are based on monthly means from June to September 1958–97, except for AIRI which is based on seasonal means of June–September 1958–95. Coefficients that are significant at the 99% confidence level are bolded. WYI, AIRI, and MHI represent the Webster and Yang index, all Indian summer rainfall index, and monsoon Hadley circulation index, respectively. MCI1 and MCI2 are WSI1 and DU2, respectively.

	WYI	**AIRI**	**MH1**	**MCI1**	**MCI2**
WYI	1.00	**0.52**	**0.29**	**0.93**	**0.35**
AIRI	**0.52**	1.00	**0.64**	**0.68**	–0.18
MHI	**0.29**	**0.64**	1.00	**0.51**	**–0.35**
MCI1	**0.93**	**0.68**	**0.51**	1.00	0.15
MCI2	**0.35**	–0.18	**–0.35**	0.15	1.00

b. Discussion

Regardless of the good correlations between CI1 and MCI1 or between CI2 and MCI2, the convection and circulation indices show large discrepancies during certain years. In 1997, for example, the seasonal-mean convection in ISM (CI1) was normal but the corresponding large-scale monsoon circulation index (MCI1) indicates a remarkably weak ISM (Fig. 7a). Inconsistency can also be found between CI1 and MCI1 in the summers of 1987, 1992, and 1994 (Fig. 7a). This seems to suggest that during the summer when strong ENSO warming occurs (such as in the summers of 1987, 1992, 1994, and 1997), the convection and westerly shear indices tend to diverge for both the monthly and seasonal-mean anomalies. The prominent ENSO warming during boreal summer appears to be one of the sources of the inconsistency between the convection and circulation indices in the ISM domain. This assertion needs to be verified using long-term records, because it may be subject to interdecadal variations. The poor relation between CI1 and MCI1 is outstanding, primarily in the recent decade.

Another notable feature is that the ISM convection index CI1 exhibits an evident interdecadal variability characterized by a rapid increase of the intensity of monsoon convection in the late 1970s and early 1980s (Fig. 7a). This regime shift, however, is not obvious in the corresponding circulation index MCI1. The interdecadal variability appears to be another source of the inconsistency between convection and circulation indices.

In contrast, in the SEASM region, the monsoon indices, CI2 and MCI2, do not show evident interdecadal variability similar to that of CI1. The large discrepancies between CI2 and MCI2 occur during the summers of 1976, 1982, 1988, 1993, and 1995 (Fig. 7b). These years include both El Niño (1976, 1982, 1993) and La Niña (1988 and 1995). The El Niño/La Niña events do not appear responsible for the divergence between convection and circulation indices in the SEASM. This may imply that the intrinsic chaotic nature of the summer monsoon may be another cause of the inconsistency between convection and monsoon indices. Further understanding of the causes of this inconsistency between convection and circulation indices is important from both theoretical and practical points of view.

Acknowledgments. This study is supported by NOAA OGP through cooperative agreement NA67RJ0154, NSF Climate Dynamics Program Grant ATM-9613776, and ONR Marine Meteorology Program N00014-96-1-0796. The authors thank Dr. T. A. Schroeder for his comments. Thanks extend to two anonymous reviewers' comments that led to a significantly improved manuscript.

References

Ailikun, B., and T. Yasunari, 1998: On the two indices of Asian summer monsoon variability and their implications. *Extended Abstracts, Int. Conf. on Monsoon and Hydrologic Cycle,* Kyongju, Korea, Korean Meteorological Society, 222–224.

Gill, A. E., 1980: Some simple solutions for heat-induced tropical circulation. *Quart. J. Roy. Meteor. Soc.,* **106,** 447–462.

Goswami, B. N., V. Krishnamurthy, and H. Annamalai, 1999: A broad scale circulation index for the interannual variability of the Indian summer monsoon. *Quart. J. Roy. Meteor. Soc.,* in press.

Gruber, A., and A. F. Krueger, 1984: The status of the NOAA outgoing longwave radiation data set. *Bull. Amer. Meteor. Soc.,* **65,** 958–962.

Huang, R.-H., and L. Lu, 1989: Numerical simulation of the relationship between the anomaly of subtropical high in east Asia and the convective activity in the tropical western Pacific. *Adv. Atmos. Sci.,* **6,** 202–214.

Kalnay, E., and Coauthors, 1996: The NCEP/NCAR 40-Year Reanalysis Project. *Bull. Amer. Meteor. Soc.,* **77,** 437–471.

Kawamura, R., 1998: A possible mechanism of the Asian summer monsoon-ENSO coupling. *J. Meteor. Soc. Japan,* **76,** 1009–1027.

Krishnamurti, T. N., H. S. Bedi, and M. Subramaniam, 1989: The summer monsoon of 1988. *Meteor. Atmos. Phys.,* **42,** 19–37.

Lau, K.-M., 1998: A climate system approach to studies of the Asian summer monsoon. *Extended Abstracts, Int. Conf. on Monsoon and Hydrologic Cycle,* Kyongju, Korea, Korean Meteorological Society, 15.

——, and P. H. Chan, 1986: Aspects of the 40–50 day oscillation during the northern summer as inferred from outgoing longwave radiation. *Mon. Wea. Rev.,* **114,** 1354–1467.

Livezey, R. E., and W. Y. Chen, 1983: Statistical field significance and its determination by Monte Carlo techniques. *Mon. Wea. Rev.,* **111,** 46–59.

Meehl, G., 1987: The annual cycle and interannual variability in the tropical Pacific and Indian Ocean region. *Mon. Wea. Rev.,* **115,** 27–50.

Nitta, T., 1987: Convective activities in the tropical western Pacific and their impact on the Northern Hemisphere summer circulation. *J. Meteor. Soc. Japan,* **65,** 373–390.

Parthasarathy, B., R. R. Kumar, and D. R. Kothawale, 1992: Indian summer monsoon rainfall indices, 1871–1990. *Meteor. Mag.,* **121,** 174–186.

Shukla, J., and D. A. Paolino, 1983: The Southern Oscillation and longrange forecasting of the summer monsoon rainfall over India. *Mon. Wea. Rev.,* **111,** 1830–1837.

——, and D. A. Mooley, 1987: Empirical prediction of the summer monsoon rainfall over India. *Mon. Wea. Rev.,* **115,** 695–703.

Sontakke, N. A., G. B. Pant, and Nityanand Singh, 1993: Construction of all-Indian summer monsoon rainfall series for the period 1844–1991. *J. Climate,* **6,** 1807–1811.

Waliser, D. E., and W. Zhou, 1997: Removing satellite equatorial crossing time biases from the OLR and HRC datasets. *J. Climate,* **10,** 2125–2146.

Wang, B., 1994: Climatic regimes of the tropical convection and rainfall. *J. Climate,* **7,** 1109–1118.

Webster, P. J., 1972: Response of the tropical atmosphere to local, steady forcing. *Mon. Wea. Rev.,* **100**, 518–541.

——, and S. Yang, 1992: Monsoon and ENSO: Selectively interactive systems. *Quart. J. Roy. Meteor. Soc.,* **118,** 877–926.

Xie, P., and P. A. Arkin, 1997: Global precipitation: A 17-year monthly analysis based on gauge observations, satellite estimates, and numerical model outputs. *Bull. Amer. Meteor. Soc.,* **78,** 2539–2558.

Yanai, M., and T. Tomita, 1998: Seasonal and interannual variability of atmospheric heat sources and moisture sinks as determined from NCEP–NCAR reanalysis. *J. Climate,* **11,** 463–482.

Yasunari, T., 1991: The monsoon year—A new concept of the climate year in the tropics. *Bull. Amer. Meteor. Soc.,* **72,** 1331–1338.

Zhu, B., and B. Wang, 1993: The 30–60-day convection seesaw between the tropical Indian and western Pacific Oceans. *J. Atmos. Sci.,* **50,** 184–199.